SICE Annual Conference 2015
July 28-30, 2015, Hangzhou, China

Development of a Wearable Gait Assist Robot using Interactive Motor Rhythmic Stimulation to Upper and Lower Limbs

Robin Miao Sin Yap, Daiki Kono, Yuriko Saruta, Hironobu Matsui, Ken-ichiro Ogawa, Yoshihiro Miyake
Department of Computational Intelligence and Systems Science
Tokyo Institute of Technology
Tokyo, Japan
Email: robin@myk.dis.titech.ac.jp
Seki Masatoshi, Ken Ichiryu
Kikuchiseisakusho Co., ltd.
Tokyo, Japan

Abstract: Ageing population is a global social problem due to increase in life expectancy and improvement in medical care. In this study, we developed a gait rehabilitation system using interactive motor rhythmic stimulation based on mutual entrainment to help elderly in walking. Mutual entrainment is a natural phenomenon that occur as a result of rhythmic interaction between two or more non-linear oscillators. During this process, the oscillator with a high frequency slows down while the oscillator with a low frequency speeds up, until both oscillators generates the same frequency. In this system, the input rhythm of human footstep timing (phase) is synchronized with the output rhythm of the upper and lower limbs' motor timing (phase) of the system. This system is expected to improve upper and lower limb coordination for elderly's gait.

Keywords: Mutual entrainment, Gait rehabilitation system, Interactive motor rhythmic stimulation, Upper and Lower Limb Coordination, Elderly's gait

1. INTRODUCTION

Ageing population is a global social problem due to increase in life expectancy. It was reported that in Japan alone, the percentage of elderly population will increase from 26.6% in 2015 to 36.4% in 2065 [1]. More developed regions also show similar trend although not as steep as compared with Japan. In terms of problems associated with elderly locomotion, age-related deterioration of coordinated interlimb behaviour has also been reported [2].

Mutual entrainment is a natural physical phenomenon that occur as a result of rhythmic interaction between two or more non-linear oscillators. The nature of coupling between segmental oscillators of the lamprey spinal generator for locomotion was investigated and a bidirectional coupling between the oscillators, which generates a stable travelling wave was found [3]. The swimming pattern of an aquatic animal and a gait pattern generator of a quadruped was studied using computer simulations and the proposed system generates some desirable pattern [4]. The coordinated movements of bipedal locomotion by global entrainment between the rhythmic activities of a nervous system, which composed of coupled neural oscillators and rhythmic movements of a musculo-skeletal system was studied using computer simulations, and walking movements stable to mechanical perturbation and environment was obtained [5].

More recently, the effects of arm swing on human locomotion was investigated experimentally and the gross and net energy expenditure were found to be significantly higher during walking without arm swing [6]. The coordination of upper and lower limb movements between healthy and stroke patients on a treadmill was investigated experimentally and stroke subjects were able to walk at a faster speed when using sliding handles to perform arm movement, suggesting the positive effects of arm movements on gait rehabilitation [7].

In terms of engineering applications, many power-assist wearable systems have also been developed to allow users to perform various functions. The HAL-3 exoskeleton was developed using electromagnetic (EMG) based feedback control to help patients in walking [8]. The medical exoskeleton eLEGS was developed to allow users to stand up, walk and sit down independently [9]. However, these approaches still remain at the stage of master-slave control and no mutual entrainment has yet to be considered.

Based on all these backgrounds, we have developed a wearable gait assist robot (Walk-Mate) using mutual entrainment as a mechanism, based on an earlier framework [10]. In this system, the input rhythm of the human footsteps' timing (phase) are synchronized with the output rhythm of the upper and lower limbs' motor timing (phase) of the user. This system is expected to improve upper and lower limb coordination for elderly's gait.

2. MATERIALS AND METHODS

2.1 Summary

2.1.1 System Appearance

The wearable robot comprises of two upper and lower limb motors. The upper limb motors are rigidly attached to the upper limb spiral-ware which can be secured to the upper limb (i.e. between elbow joint and shoulder joint) using elastic strap. Similarly, the lower limb motors are rigidly attached to the lower limb spiral-ware which can be secured to the lower limb (i.e. between knee joint and hip joint) using elastic strap. The system can be secured to the upper body (i.e. chest) and lower body (i.e. abdominal region) using adjustable belts. Fig.1 shows the appearance of the wearable robot.

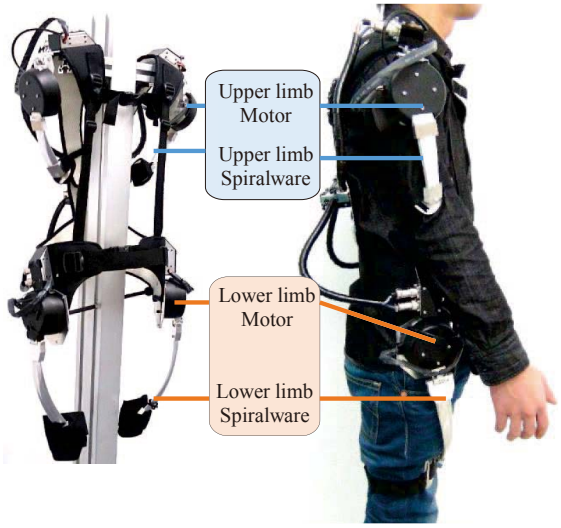

Fig.1 Appearance of wearable robot.

2.1.2 Overall System Architecture

There are two main modules for the wearable robot (Walk-Mate), namely hardware module and software module. Fig. 2 shows the schematic diagram of the hardware module of Walk-Mate. The hardware module comprises of three main modules, namely actuator module, sensor module and control module. The actuator module comprises of two upper limb motors and two lower limb motors. The sensor module comprises of one left foot sensor and one right foot sensor. The control module comprises of one PC, two I/O units, one power unit and four motor controllers. Fig. 3 shows the schematic diagram of the software module of Walk-Mate. The software module comprises of three main modules, namely mutual entrainment module, upper and lower limb timing control module and motor torque control module. The input signal from the left foot sensor, $\Delta\theta_{hl}$ and right foot sensor, $\Delta\theta_{hr}$ is sent to the mutual entrainment module, which comprises of two main modules, namely module-1 (mutual entrainment) and module-2 (phase control). The phase control module converges the phase difference between the human walking timing (i.e. phase) with the upper and lower limb motor timing (i.e. phase), $\Delta\theta_m$ to the target phase difference, $\Delta\theta_d$. Module-3 (Motor timing control) controls the phase difference between the upper limb motor, $\Delta\theta_{mu}$ and lower limb motor, $\Delta\theta_{ml}$. Module-4 (Motor torque control) controls the motor torque output to the upper and lower limb based on the output motor timing to the upper and lower limb.

2.2 Hardware

2.2.1 Hardware Framework

The hardware comprises of three main modules, namely actuator module, sensor module and control module. The actuator module comprises of two upper limb motors and two lower limb motors. The sensor module comprises of one left foot sensor and one right foot sensor. The control module comprises of one PC, two I/O unit, one power unit and four motor controllers. Fig. 4 shows the hardware configuration of the hardware module.

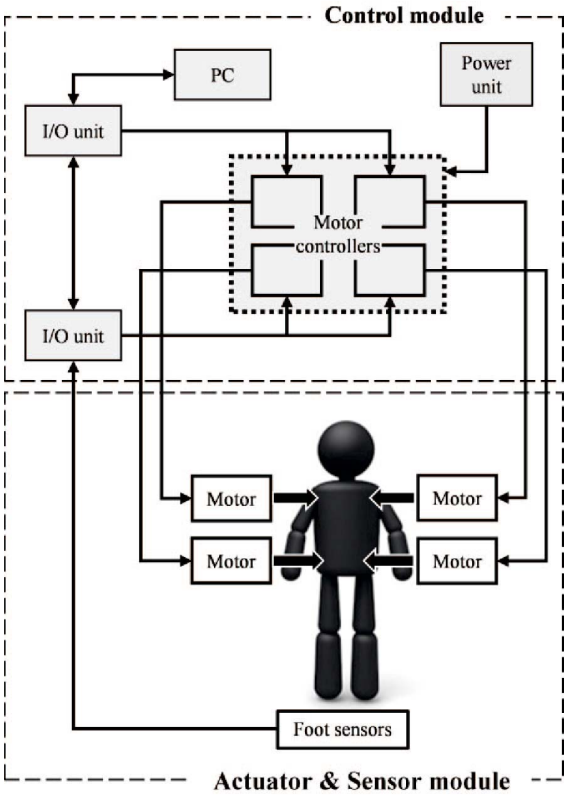

Fig.2 Schematic diagram of hardware module.

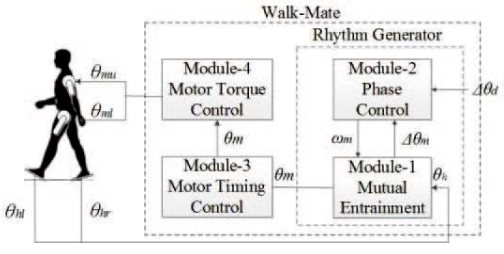

Fig.3 Schematic diagram of software module.

2.2.2 Actuator module

The actuator module comprises of two upper limb motors and two lower limb motors. The upper limb motor is rigidly attached to the upper limb spiral ware. The upper limb spiral ware is ergonomically designed which can be secured to the upper limb (i.e. between elbow joint and shoulder joint) via elastic straps. Similarly, the lower limb motor is rigidly attached to the lower limb spiral ware which can be secured to the lower limb (i.e. between knee joint and hip joint) via elastic straps. The upper and lower limb motors are DC motors which are primarily driven using pulse-width modulation (PWM) duty, hence does not have any form of feedback control. The maximum voltage of the motors are ±5.0V. A positive voltage provides a forward torque, whereas a negative voltage provides a reverse torque. Each motor is controlled by one motor controller which comprises of a D/A (digital to analogue) converter (Analogue Devices, DAC08, USA).

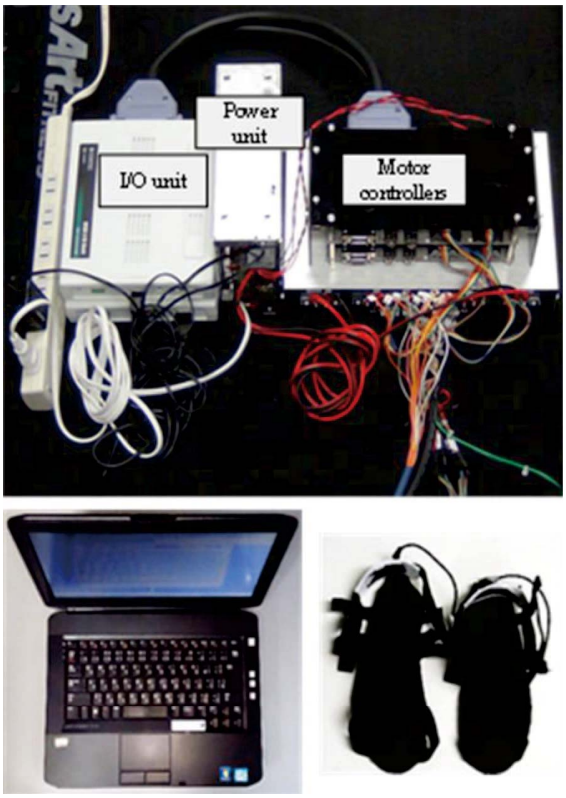

Fig.4 Hardware configuration of hardware module.

2.2.3 Sensor module

The foot sensor (OJIDEN, OT-21BP-G, Japan) is an elongated tape switch sensor which is inserted into the shoe-pad placed below the shoe. The tape switch will make contact when the user's footstep come into contact with the ground. The output jack of the foot sensor is connected to the I/O of the motor controller. The shoe-pad is rigidly secured to the shoe via elastic straps with Velcro.

2.2.4 Control module and power unit

The control module comprises of one PC (DELL, E5430, USA), two I/O unit (CONTEC, DIO-1616LX-USB, Japan), four motor controllers, one power unit (COSEL, PBA600F-24, Japan) and cables. The power unit is driven by external electrical supply.

2.3 Software

2.3.1 Software Framework

The software module comprises of three main modules, namely mutual entrainment module, upper and lower limb motor timing control module and motor torque control module.

2.3.2 Mutual entrainment module

The mutual entrainment module comprises of two main modules, namely module-1 (mutual entrainment) and module-2 (phase control). Module-1 has a couple of non-linear phase oscillators based on the Kuramoto model [11] described as

$$\dot{\theta}_{m,l} = \omega_{m,l} + K_{lr}\sin(\theta_{m,r} - \theta_{m,l}) + K_m \sin(\Delta\theta_{m,l} - \Delta\theta_d), \quad (1)$$

$$\dot{\theta}_{m,r} = \omega_{m,r} + K_{lr}\sin(\theta_{m,l} - \theta_{m,r}) + K_m \sin(\Delta\theta_{m,r} - \Delta\theta_d), \quad (2)$$

where $\Delta\theta_{m,l} = \theta_{h,l} - \theta_{m,l}$, $\Delta\theta_{m,r} = \theta_{h,r} - \theta_{m,r}$.

Here, $\omega_{m,l}$, $\omega_{m,r}$ is the natural frequency of left and right motor output rhythm respectively. $\theta_{m,l}$, $\theta_{m,r}$ is the phase of motor output rhythm to left and right lower limb respectively, and $\theta_{h,l}$, $\theta_{h,r}$ is the phase of human walking input rhythms to the left and right lower limbs respectively. Also, K_{lr} is the coupling constant between the left and right lower limb motors of the system, and K_m is the coupling constant between a human and the robot.

Module-2 serves as a control module for the natural frequencies, $\omega_{m,l}$, $\omega_{m,r}$ to rapidly converge the phase differences, $\Delta\theta_{m,l}$ and $\Delta\theta_{m,r}$ to the target phase difference, $\Delta\theta_d$ using the following equations,

$$\dot{\omega}_{m,l} = \varepsilon \sin(\Delta\theta_{m,l} - \Delta\theta_d), \quad (3)$$

$$\dot{\omega}_{m,r} = \varepsilon \sin(\Delta\theta_{m,r} - \Delta\theta_d). \quad (4)$$

Here, ε is the control gain ($\varepsilon > 0$) and $\Delta\theta_d$ is the target phase difference. In this study, we set $\omega_{m,l} = 4.0$ rad/s, $\omega_{m,r} = 4.0$ rad/s, $K_{lr} = 5.0$, $K_m = 0.5$, $\varepsilon = 0.16$ and $\Delta\theta_d = 0$. Also, we initialize the human left and right walking phase, θ_{hl} and θ_{hr} as 0 and π respectively, and robot left and right walking phase, θ_{ml} and θ_{mr} as 0. The mutual entrainment relationship between human and Walk-Mate is illustrated in Fig.5.

Fig. 6 shows the schematic diagram of the Walk-Mate control algorithm. The Walk-Mate control algorithm is a three-step process, namely step-1 (initialization phase), step-2 (human footstep detection phase) and step-3

(mutual synchronization of robot and human walking phase). During the initialization phase, the robot left and right walking phase, θ_{ml} and θ_{mr} is initialized with the human left and right walking phase, θ_{hl} and θ_{hr} as 0 and π respectively. During the human footstep detection phase, the natural frequency of the robot left walking phase, ω_{ml} and right walking phase, ω_{mr} is updated such that the left and right walking phase difference between human and robot converges to the target difference, $\Delta\theta_d$. Finally, during the mutual entrainment of human and robot walking phase, the updated natural frequency of robot is used to synchronize the human walking phase with the robot walking phase.

As a form of safety precaution, the motor starts moving after four complete gait cycle to prevent the user from injury due to sudden jerking movement of the motors. Also, the motors come to a stop 1.5 seconds after the human stops walking to prevent excessive motor movement which may cause injury to the user.

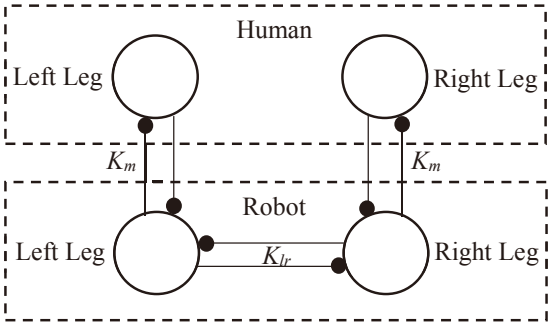

Fig.5 Schematic diagram of mutual entrainment between human and robot.

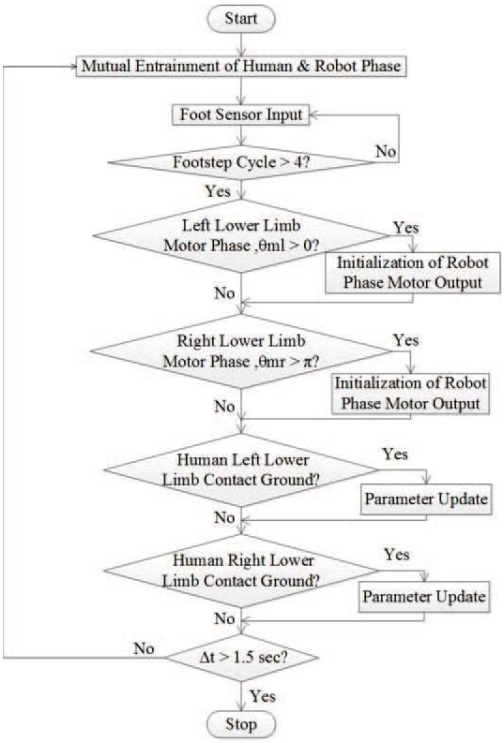

Fig.6 Flow chart of Walk-Mate control algorithm.

2.3.3 Upper and Lower Limb Motor Timing Control Module

We first conducted a preliminary experiment to investigate the natural timing (phase) difference between the foot contact timing (phase) and arm swing of upper limb during natural human locomotion. Six healthy human subjects participated in this preliminary investigation. Out of six subjects, four are male (age: 24.3 ± 1.72 years; height: 170.8 ± 7.84 cm; weight: 73 ± 7.26 kg) and two are female (age: 27 ± 2.82 years; height: 155.5 ± 3.54 cm; weight: 46 ± 1.41 kg). All the participants were instructed to walk on a treadmill (SportsArt Fitness, T650MES, Japan) at their natural walking speed for about 1 minute. Before the start of the experiment, the comfortable walking speed of each participants were confirmed. Each subjects walked on the treadmill for about 10 sec. The kinematics of the right upper and lower limbs of each subjects were captured using 3D motion capture system (Nobby Tech, VENUS 3D, Japan), together with six infra-red cameras positioned on the right hand side of the subjects. Six reflection markers (three on right upper limb and three on right lower limb) were placed on the human subjects. The position of the markers on the right upper limb were as follows: outer region of shoulder joint; elbow joint; and wrist. The position of the markers on the right lower limb were as follows: outer region of pelvic joint; knee joint; and ankle joint. Fig. 7 shows the schematic diagram of the experiment set-up and position of reflection markers on the subject.

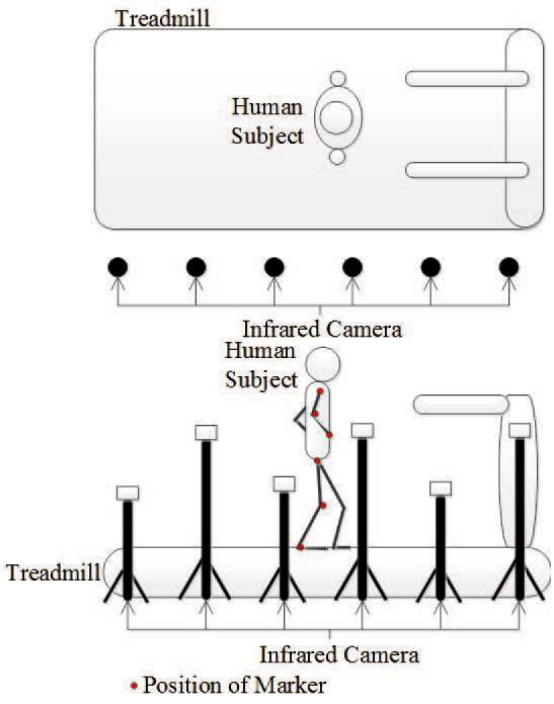

Fig.7 Schematic diagram of experiment set-up for timing analysis of foot contact timing and upper limb arm swing.

Fig 8 shows the plot of angular displacement of the right upper limb versus time, and vertical displacement of the right ankle versus time for four complete human gait cycles. The left and right vertical axis shows the right ankle vertical displacement and right upper limb angular displacement respectively. The angular displacement of the right upper limb was measured with respect to the rest position at 0 deg. The vertical displacement of the right ankle was measured with respect to the height of the treadmill 0.32m from the ground. The results showed that there is a time lag between the right upper limb angular displacement and the foot contact for the forward and backward arm swing phase. We calculated the mean value of the time lag during the forward swing and backward swing phase for six subjects and the results were tabulated as shown in Table 1. The mean time-lag for the forward arm swing and backward arm swing with respect to the foot contact timing, which was calculated as a percentage of one complete gait cycle are 17.6 ± 2.7% and 66.5 ± 3.3% respectively. The results showed that when the right foot comes into contact with the ground, the right upper limb does not immediately come to a rest position. Instead, there exist a forward and backward time-lag of 15~20% and 60~ 70% of one complete gait cycle respectively. Therefore, we take the forward and backward time-lag into consideration in the software development of the upper and lower limb motor timing control module.

Table 1: Mean value and standard deviation of time lag between right foot contact phase, and rest position of right upper limb during forward and backward arm swing phase for one complete gait cycle expressed as a percentage and radian.

	lag_fwd/ %	lag_fwd/ rad	lag_bwd/ %	lag_bwd/ rad
Sub 1	19.9	1.25	67.6	4.25
Sub 2	15.1	0.95	65.6	4.12
Sub 3	17.2	1.08	70.2	4.41
Sub 4	21.5	1.35	63.6	3.99
Sub 5	14.4	0.90	62.3	3.91
Sub 6	17.7	1.11	69.4	4.36
Mean	17.6	1.11	66.5	4.17
S.D	2.7	0.17	3.3	0.20

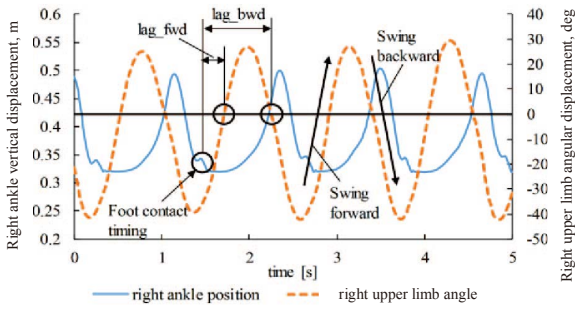

Fig.8: Time lag analysis of right foot contact timing and right upper limb arm swing.

The timing control between the upper and lower limb motors is based on the natural human locomotion using the following assumptions: The right upper and lower limb; and left upper and lower limb are 180° out of phase (i.e. anti-phase). The right upper limb and left lower limb; and left upper limb and right lower limb are in phase. Fig. 9 shows the phase diagram of the left and right upper limb and left and right lower limb with respect to the foot contact timing for one complete gait cycle.

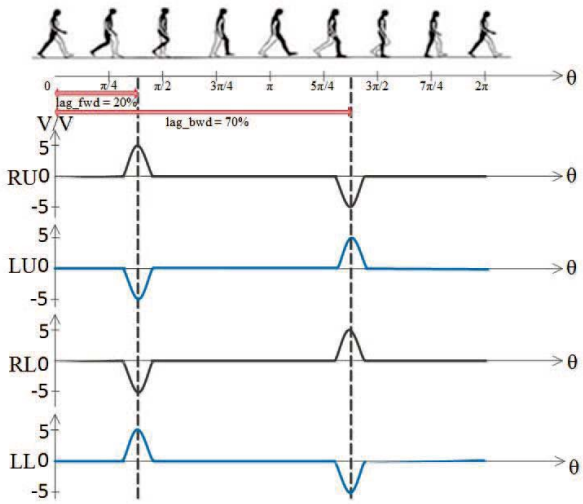

Fig.9: Phase diagram of left and right upper limb, and left and right lower limb with respect to the foot contact timing for one complete gait cycle (RU: Right upper limb; LU: Left upper limb; RL: Right lower limb; LL: Left lower limb) .

2.3.4 Motor Torque Control Module

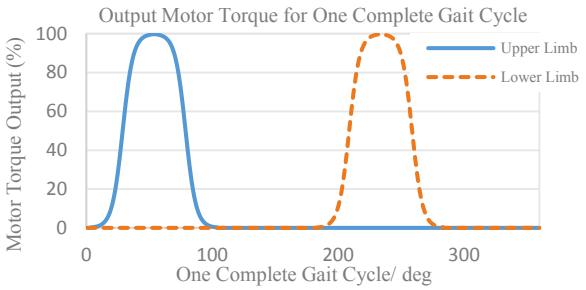

Fig.10 Output motor torque to upper and lower limb for one complete gait cycle.

We used the timing relationship between the foot contact timing and upper and lower limb motor timing (phase) to control the motor output torque. The onset of the peak motor torque output to the upper limb corresponds to the forward time-lag of 20%. The onset of the peak motor torque of the lower limb corresponds to the backward time-lag of 70%. The increasing and decreasing function of the upper and lower limb motor torque is

modelled using the sigmoid function and inverse sigmoid function respectively described as:

$$S_U(t) = \frac{1}{1+e^{-kt}} \times 100, \quad (5)$$

$$S_D(t) = \frac{1}{1+e^{kt}} \times 100, \quad (6)$$

where S_U = Increasing function, S_D = Decreasing function, $-1 \leq t \leq 1$, $k = 6$. Fig. 10 shows a typical plot of the upper and lower limb motor torque expressed as a percentage for one complete gait cycle using the sigmoid function.

3. SYSTEM EVALUATION

Finally, we evaluated the system with five healthy elderly subjects (three males and two females). Each subject put on the wearable robot and walked along a smooth corridor of 55 m under two different experiment conditions, namely assist and non-assist condition. For the non-assist condition, there is no output motor torque to the upper and lower limb. For the assist condition, there is an output motor torque to the upper and lower limb with an input time-lag of 15% between the foot contact timing and upper limb motors. We evaluated the angular displacement of the shoulder joint and hip joint under the two different experiment conditions using encoder data obtained from the upper and lower limb motor of the wearable robot. We calculated the mean value of the amplitude of the shoulder joint and hip joint angle for five complete gait cycles and the result is shown in Fig. 11. The results showed that under non-assist and assist condition, there is an increase in the shoulder joint and hip joint angle from 24.9° to 40.5°, and 39.2° to 44.1° respectively. The increase in the shoulder joint angle is more significant as compared with the hip joint angle.

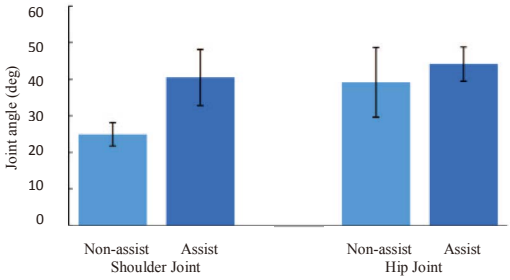

Fig.11 Mean value of shoulder and hip joint angle under assist and non-assist condition.

4. CONCLUSION

In conclusion, we have developed a wearable robot using interactive motor rhythmic stimulation to upper and lower limb. We evaluated the effectiveness of the system with five elderly subjects and found a significant increase in the shoulder joint angle as compared with the hip joint angle under assist condition. The increase in shoulder joint angle is desirable as it improves the efficiency of the gait dynamics in human locomotion [6, 7]. We have also evaluated the effectiveness of the system for elderly's gait stability. However, due to space constraint, we will not present the results in this paper. As an extension of this present framework, we will continue to develop the system and evaluate its effectiveness for upper and lower limb coordination with elderly.

REFERENCES

[1] World Populations Prospects: The 2012 Revision http://esa.un.org/wpp/index.htm.

[2] Van Emmerik, R.E.A., McDermott, W.J., Haddad, J.M., Van Wegen, E.E.H., "Age-Related Changes in Upper Body Adaptation to Walking in Human Locomotion", *Gait and Posture*, Vol. 22, pp. 233-239, 2005.

[3] Cohen, A.H., Holmes, P.J., Rand, R.H., "The Nature of the Coupling Between Segmental Oscillators of the Lamprey Spinal Generator for Locomotion: A Mathematical Model", *Journal of Mathematical Biology*, Vol. 13, pp. 345-369, 1982.

[4] Yuasa, H., Ito, M., "Coordination of Many Oscillators and Generation of Locomotory Patterns", *Biological Cybernetics*, Vol. 63, pp. 177-184, 1990.

[5] Taga, G., Yamaguchi, Y., Shimizu, H., "Self-organized Control of Bipedal Locomotion by Neural Oscillators in Unpredictable Environment", *Biological Cybernetics*, Vol. 65, pp 147-159, 1991.

[6] Umberger, B.R., "Effects of Suppressing Arm Swing on Kinematics, Kinetics, and Energetics of Human Walking", *Journal of Biomechanics*, Vol. 41, pp. 2575-2580, 2008.

[7] Stephenson, J.L., Lamontagne, A., De Serres, S.J., "The Coordination of Upper and Lower Limb Movements During Gait in Healthy and Stroke Individuals", *Gait and Posture*, Vol. 29, pp 11-16, 2009.

[8] Kawamoto, H., Lee, S., Kanbe, S., Sankai, Y. "Power Assist Method for HAL-3 using EMG-based Feedback Controller," *Proceedings of International Conference on of International Conference on Systems, Man and Cybernetics* (SMC2003), pp. 1648-1653, 2003.

[9] Strausser, K. A., Kazerooni, H., "The Development and Testing of a Human Machine Interface for a Mobile Medical Exoskeleton", *IEEE/RSJ International Conference on Intelligent Robots and Systems*, San Francisco, CA, USA, pp. 4911-4916, 2011.

[10] Miyake, Y., "Interpersonal Synchronization of Body Motion and the Walk-Mate Walking Support Robot", *IEEE Transactions on Robotics*, Vol. 25, No. 3, pp. 638-644, 2009.

[11] Kuramoto, Y., Chemical Oscillation, waves and turbulence, Springer-Verlag, 1984.